Old trees bloom new flowers, lysosome targeted near-infrared fluorescent probe for ratiometric sensing of hypobromous acid in vitro and in vivo based on Nile red skeleton

Wanqing Zhao, Pengyue Xu, Yixuan Ma, Yiming Song, Yihang Wang, Panpan Zhang, Bin Li, Yongmin Zhang, Jianli Li, Shaoping Wu

▶ **To cite this version:**

Wanqing Zhao, Pengyue Xu, Yixuan Ma, Yiming Song, Yihang Wang, et al.. Old trees bloom new flowers, lysosome targeted near-infrared fluorescent probe for ratiometric sensing of hypobromous acid in vitro and in vivo based on Nile red skeleton. Bioorganic Chemistry, 2024, 143, pp.107031. 10.1016/j.bioorg.2023.107031 . hal-04344732

HAL Id: hal-04344732

https://hal.sorbonne-universite.fr/hal-04344732

Submitted on 14 Dec 2023

HAL is a multi-disciplinary open access archive for the deposit and dissemination of scientific research documents, whether they are published or not. The documents may come from teaching and research institutions in France or abroad, or from public or private research centers.

L'archive ouverte pluridisciplinaire **HAL**, est destinée au dépôt et à la diffusion de documents scientifiques de niveau recherche, publiés ou non, émanant des établissements d'enseignement et de recherche français ou étrangers, des laboratoires publics ou privés.

Old trees bloom new flowers, lysosome targeted near-infrared fluorescent probe for ratiometric sensing of hypobromous acid in vitro and in vivo based on Nile red skeleton

Wanqing Zhao[a], Pengyue Xu[a], Yixuan Ma[a], Yiming Song[c,*], Yihang Wang[a], Panpan Zhang[a], Bin Li[a], Yongmin Zhang[a,d], Jianli Li[b], Shaoping Wu[a,*]

[a] *Key Laboratory of Resource Biology and Biotechnology in Western China, Ministry of Education, Biomedicine Key Laboratory of Shaanxi Province, Northwest University, 229 Taibai Road, Xi'an, Shaanxi, 710069, P. R. China.*

[b] *Key Laboratory of Synthetic and Natural Functional Molecule Chemistry of the Ministry of Education, College of Chemistry and Materials Science, Northwest University, Xi'an, 710069, P. R. China.*

[c] *School of Chemical Engineering, Northwest University, 229 Taibai Road, Xi'an, Shaanxi, 710069, P. R. China.*

[d] *Sorbonne Université, CNRS, Institut Parisien de Chimie Moléculaire, UMR 8232, 4 place Jussieu, 75005, Paris, France.*

[*] *Corresponding author.*

E-mail addresses: ymsong@nwu.edu.cn (Y. Song), wushaoping@nwu.edu.cn (S. Wu).

Abstract

Hypobromous acid (HOBr), one of the significant reactive oxygen species (ROS) that acts as an important role in human immune system, however the increasing level of HOBr in human body can cause the disorder of eosinophils (EPO), leading to oxidative stress in organelles, and further causing a series of diseases. In this study, a ratiometric fluorescent probe **DMBP** based on Nile red skeleton was developed to detect HOBr specifically by the electrophilic substitution with HOBr. **DMBP** emits near-infrared (NIR) fluorescence at 653 nm, after reacting with HOBr, the emission wavelength of **DMBP** shifted blue and a new peak appeared at 520 nm, realizing a ratiometric examination of HOBr with a limit of detection of 89.00 nM. Based on its sensitive and specific response to HOBr, **DMBP** was applied in the visual imaging of

HOBr in HepG2 cells and zebrafish. Foremost, probe **DMBP** has excellent lysosome targeting ability and NIR emission reduced the background interference of biological tissues, providing a potential analytical tool to further investigate the role of HOBr in lysosome.

Keywords: Near infrared; Fluorescent probe; HOBr; Lysosome; Bioimaging

1. Introduction

Reactive oxygen species (ROS) are a class of oxygen-containing chemically reactive substances that are indispensable in cell signaling and maintenance of homeostasis in the body [1-3]. Hypobromic acid (HOBr) is one of the significant ROS which is generated by hydrogen peroxide and bromine ion catalyzed by eosinophils (EPO) in the human immune system [4-6]. HOBr possesses strong oxidizing and halogenating capabilities and therefore participates in a host of biological processes in the human defense system, like anti-inflammation, sterilization and resistance to pathogen invasion [7, 8]. However, the overexpression levels of HOBr in the body can lead to EPO disorders, which can result in oxidative stress in cellular organelles and further trigger a variety of physiopathological reactions, such as tissue injury, rheumatoid arthritis, cardiovascular diseases and cancers [9-11]. Therefore, the detection of HOBr level in vivo and vitro is crucial in clinical practice. In addition, lysosome is a main organell of ROS production, and participates in the above processes [12, 13], hence it is essential to detect the level of HOBr in lysosome to

investigate its function in physiological processes[14]. However, there are relatively few methods to detect HOBr in lysosome, it is still a challenge to develop a novel method to monitor HOBr level in real time.

In recent years, fluorescent probe has rapidly entered the horizons of researchers due to its high sensitivity, good selectivity, real-time monitoring and non-invasive imaging, and has become an indispensable tool for monitoring small molecular substances in vivo and in vitro [15-20]. At present, the specific detection of HOBr based on fluorescent probe still faces great challenge for two reasons: (i) the low level of HOBr in vivo (2.00~100.00 μM). (ii) the oxidation capacity of HOBr is much weaker than HOCl and is seriously susceptible to interference by other ROS [21, 22]. Therefore, there are relatively few fluorescent probes reported for the detection of HOBr. Han group firstly reported two redox fluorescent probes **mCy-TemOH** and **Cy-TemOH**, which can achieve ratiometric and quenching detection of HOBr, respectively, developed a new strategie for the detection of HOBr [23]. Kim group designed a BODIPY-based J-aggregating probe and utilized its electrophilic bromination to achieve the selective detection of HOBr generated by EPO [24], which was a pioneering work for the detection of HOBr by electrophilic substitution strategy. Overall, there are three detection mechanisms of fluorescent probe reported for HOBr detection [25]: (i) oxidation reaction caused by HOBr as a strong oxidant [26], (ii) HOBr-catalyzed coupling cyclization of amino groups with sulfur-methyl group [27], (iii) electrophilic substitution reaction of HOBr and small molecular compounds [28, 29]. These sensing strategies were applied to design HOBr fluorescent probes based

on various fluorophores. In fact, in previous studies, the electrophilic halogenation of HOBr to electron-rich aromatic substrates showed stronger response than ClO^- [30, 31], and thus highly electrophilic properties of HOBr could be exploited to design its specific fluorescent probe.

Nevertheless, most of the HOBr fluorescent probes built on the aromatic bromination strategy were signal-off type owning to the intramolecular heavy atom impact [25] (Fig. 1A), and such probes are unattractive for the detection of HOBr, thus we are committed to finding a fluorophore with excellent properties to solve this problem. Fortunately, in this paper, we found that nile red would not be quenched by HOBr, on the contrary, the bromination could cause a ratiometric change in fluorescence properties of nile red to realize a ratiometric detection of HOBr. This discovery opens up a new idea for researchers to subsequently develop promising HOBr fluorescent probes.

In this work, we developed a NIR fluorescence probe **DMBP** built on nile red skeleton (Fig. 1B). **DMBP** has an electron donor N, N-diethyl and receptor carbonyl that form ICT effect, which dominated the intense red fluorescence, and has a specific site for the detection of HOBr through electrophilic substitution reaction, which changed the optical properties of **DMBP**. Probe **DMBP** emits strong red fluorescence (653 nm) at prime, then the emission wavelength shifts to 520 nm after the addition of HOBr, achieving a ratiometric fluorescence response to HOBr. Moreover, probe **DMBP** has excellent selectivity and has been applied for visual imaging of HOBr in cells and zebrafish. Furthermore, **DMBP** can localize to lysosomes and realize the

ratio detection of HOBr in lysosomes.

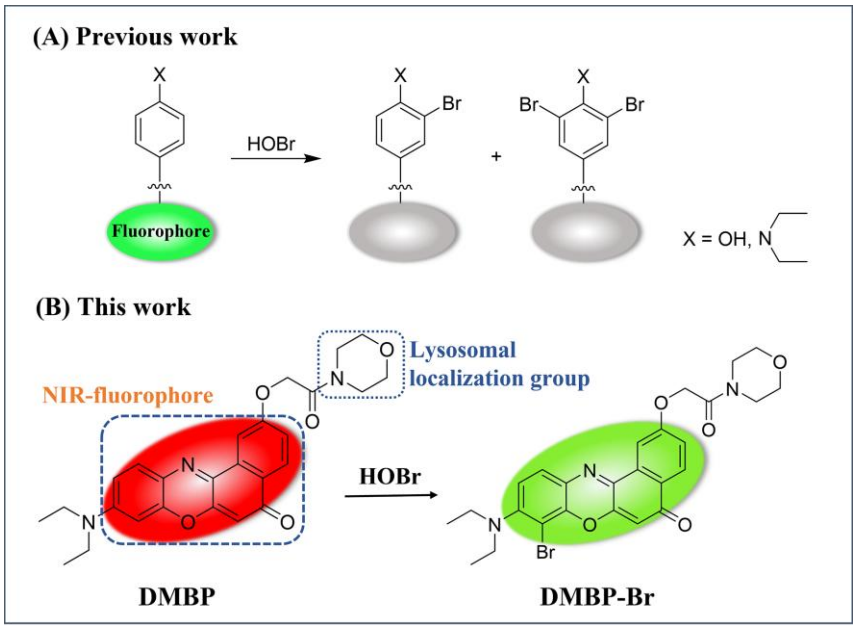

Fig. 1. Design strategy of probe **DMBP**.

2. Experimental Section

2.1. Materials and Instruments

All solvents in the experiments were of analytical grade, water was treated by an ultra-water purification system, chemical reagents were purchased from Energy Chemical, and Lyso-Tracker Green was purchased from Beyotime Biotechnology. Fluorescence spectra were obtained by F-7000 fluorescence spectrophotometer and ultraviolet spectra were acquired from UV-1880 UV-Visible spectrophotometer. Confocal images were performed with a Leica TCS SP8 laser confocal microscope. The MS and NMR data were obtained by MicroTOF QII mass spectrometer and 6001541ASP superconducting NMR instrument, respectively. Liquid chromatogram was obtained by LC-2030Plus high performance liquid chromatography system.

*2.2. Synthesis of **DMBP***

Detailed synthesis method was described in Supporting Information (Scheme S1),

and the structure of **DMBP** was determined by MS (Fig. S4), ^{1}H NMR (Fig. S6) and ^{13}C NMR (Fig. S7).

2.3. Spectral measurement

Transferred 11.5 mg **DMBP** into a 25.00 mL volumetric bottle, and fixed it with DMSO to prepare the reserve solution, then 50.00 μL of **DMBP** (1.00 mmol/L), ion solutions, 1.00 mL of DMSO and 1.00 mL of PBS solution were added to the colorimetric tube in order, then fixed with deionized water to 5.00 mL. The excitation and emission slit widths of the fluorescence spectra were 5 nm and 10 nm respectively, and the voltage was 700 V. The ion solutions used in the experiments were prepared ready-to-use, and the detailed preparation methods were described in Supporting Information. All optical spectra were scanned at room temperature.

2.4. Cell imaging experiment

Cell imaging experiments were performed with HepG2 cells. Firstly, the cytotoxicity of probe **DMBP** was detected by MTT assay, and then the imaging experiment was carried out. Detailed experimental procedures were described in Supporting Information.

2.5. Zebrafish imaging experiment

All zebrafish used in the experiments were in accordance with international ethical guidelines, and the three-day fertilized AB genotype zebrafish was selected as the experimental model. Detailed experimental procedures were described in Supporting Information.

3. Results and Discussion

*3.1. Design of probe **DMBP***

We aimed to construct a ratiometric sensing platform to detect HOBr in lysosome. Redox reaction has been considered as a feasible strategy for detecting ROS, however, it is difficult to be adopted to detect HOBr because HOBr has similar character, weaker oxidation capacity and lower concentration compared to ClO^- in vivo [32, 33], which may cause non-negligible influence. Literatures reported that electrophilic halogenation of electron-rich aromatic substrates or olefins by HOBr shows stronger reactivity than ClO^-. Mainly because Br^- is formed as an intermediate in these reactions, compared with Cl^-, Br^- has lower electronegativity and higher polarizability, making it more receptive to positive charges, and thus HOBr exhibits higher electrophilicity [24, 34]. Therefore, the high electrophilic property of HOBr can be used to design its specific fluorescent probe. As a classical NIR fluorescent dye, nile red has excellent properties such as low background interference, deep tissue penetration and good photostability [35-37], and most importantly, the aromatic ring contained in nile red can react with HOBr through electrophilic substitution, which is an ideal fluorophore for the design of HOBr fluorescent probe. In our design strategy (Fig. 1B), Nile red scaffold is used as the fluorophore, the morpholine ring as the lysosomal localization group [38, 39], and the aromatic ring in molecule can react with HOBr to generate brominated products by electrophilic substitution, which can inhibit the intramolecular charge transfer (ICT) of probe **DMBP** (the synthesis route was shown in Scheme 1, yield: 27.2%), thus affecting the spectral properties of probe **DMBP** to produce a ratiometric fluorescence response.

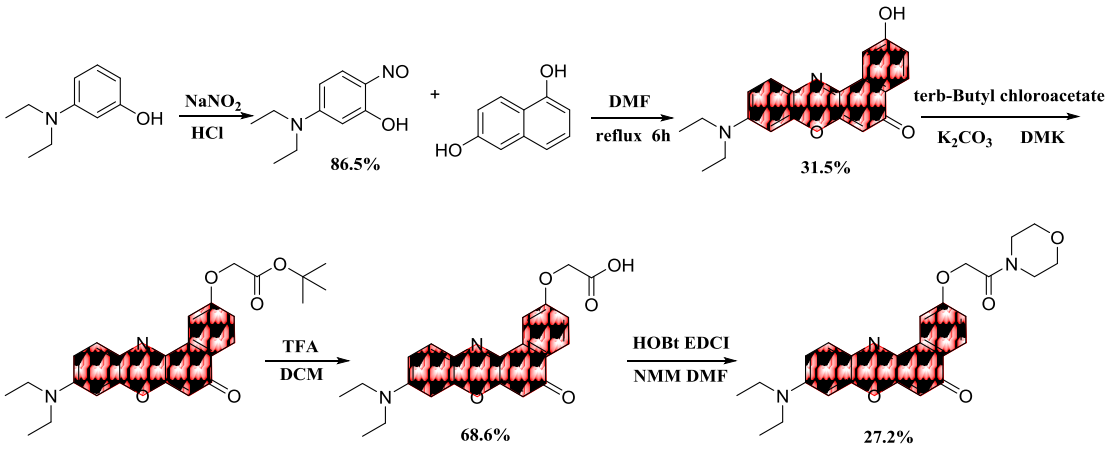

Scheme 1. Synthetic route of probe **DMBP**.

*3.2. Spectral properties of **DMBP***

Firstly, the molar absorption coefficient, fluorescence quantum yield and other related spectral properties of probe **DMBP** were measured in different organic solvents (Table S3). **DMBP** has NIR emission (653 nm) and high fluorescence quantum yield up to 30.00%, with deep tissue penetration and low background, which demonstrated its broad prospect in biological imaging. Then we examined the absorption and emission spectra of **DMBP** before and after the reaction with HOBr. The absorption and emission peaks of **DMBP** were at 580 nm and 653 nm respectively (Fig. 2A, 2B). The absorption peak at 580 nm was decreased significantly after the addition of HOBr, accompanied by an increasing peak at 420 nm (Fig. 2A). Meanwhile, the ratio changes appeared in the fluorescence spectra, the emission peak at 653 nm decreased together with an arising emission peak at 520 nm after the reaction between **DMBP** and HOBr (Fig. 2B). Selectivity and competition studies were used to demonstrate the specificity of **DMBP** to HOBr, the above results showed that other biologically relevant analytes, common anions and cations in humans would not cause ratiometric response of **DMBP** or influence the detection of

HOBr (Fig. 2C, 1D), indicating that **DMBP** has excellent selectivity for HOBr and powerful anti-interference ability.

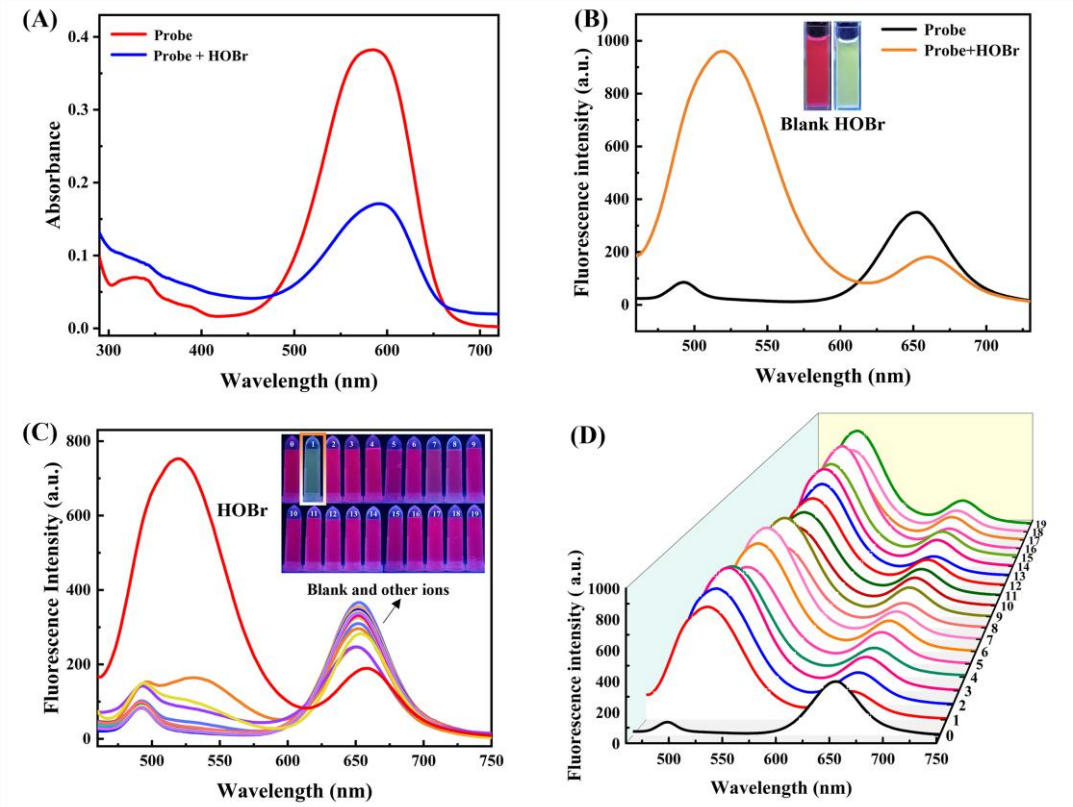

Fig. 2. (A) UV absorption spectra before and after the reaction of **DMBP** with HOBr. (B) Fluorescence emission spectra before and after the reaction of **DMBP** with HOBr. (C) Fluorescence spectra of **DMBP** (10.00 μM) upon addition of 40.0 μM 19 kinds of ions (0: blank; 1: HOBr; 2: H_2O_2; 3: ClO^-; 4: NO; 5: $ROO^·$; 6: •OH; 7: $^1O_2$; 8: $ONOO^-$; 9: *t*-BuOOH; 10: GSH; 11: Cys; 12: Hcy; 13: S^{2-}; 14: K^+; 15: Ca^{2+}; 16: Mg^{2+}; 17: Fe^{2+}; 18: Br^-; 19: NO_2^-). (D) Competitive fluorescence spectra of **DMBP** (10.0 μM) with HOBr and other biologically relevant species. λ_{ex} = 420 nm. Insets in (B): Pictures of before and after the reaction of **DMBP** with HOBr under 365 nm excitation. Insets in (C): Pictures of **DMBP** upon treatment with various ions under 365 nm excitation.

The impact of HOBr concentration on the spectral properties of **DMBP** was next investigated. Fig. 3A showed the variation trend, the increasing concentration of HOBr caused rising fluorescence intensity at 520 nm (green) and reducing at 653 nm (red) of **DMBP**. The ratio of green to red fluorescence intensity of **DMBP** was proportional to HOBr (0~56.00 μM), whose correlation index reached 0.9911 and possessed a lower Limit of Detection (LOD) of 89.00 nM (Fig. 3B). The above

experimental results indicated that **DMBP** could response to different concentrations of HOBr selectively and showed a ratiometric variation, rendering **DMBP** an ideal probe for the sensitive and accurate detection of HOBr.

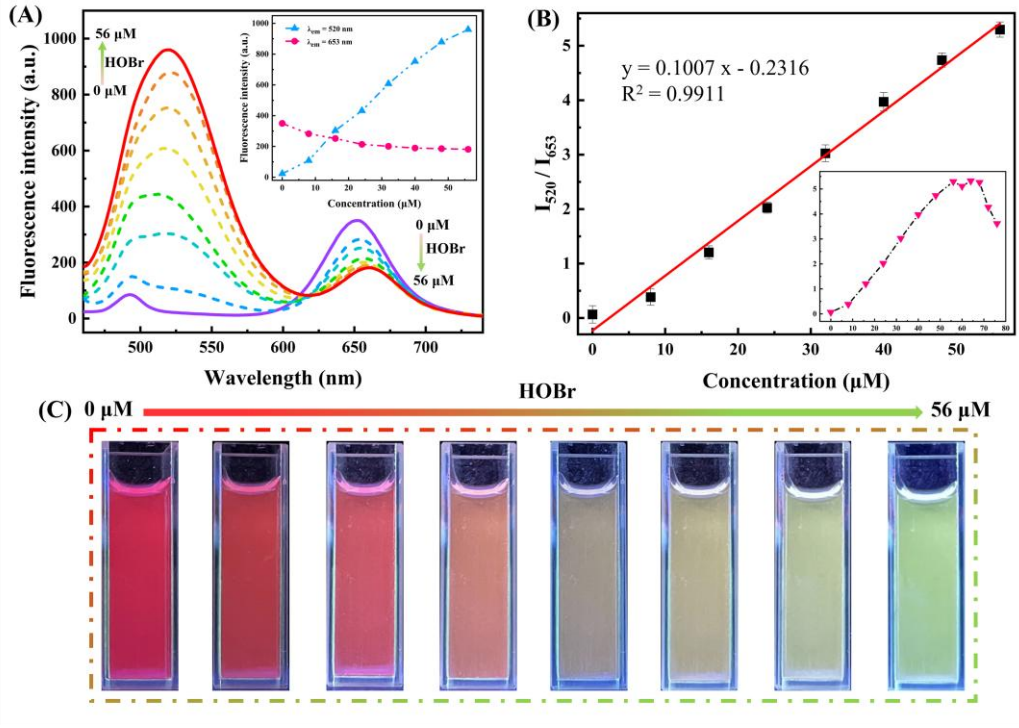

Fig. 3. (A) Fluorescence emission curves of **DMBP** (10.00 μM) with added HOBr (0~56.00 μM) (pH 7.4，20% DMSO); slit widths: 5/10 nm; operating voltage: 700 V; λ_{ex} = 420 nm. (B) Linear correlation of (A). (C) Fluorescence photos (λ_{ex} =365 nm) of probe **DMBP** after reacting with HOBr (0 μM, 8.00 μM, 16.00 μM, 24.00 μM, 32.00 μM, 40.00 μM, 48.00 μM, 56.00 μM). Inset in (A): Fluorescence intensity changes at 653 nm and 520 nm. Inset in (B): Fluorescence intensity ratio (I_{520}/I_{653}) with added HOBr (0~76.00 μM).

We also explored the effects of time and pH to examine the dynamics and pH tolerance of **DMBP** and its response to HOBr (Fig. S12). Firstly, the kinetic properties between **DMBP** and HOBr were investigated (Fig. S12A), after the addition of HOBr, the fluorescence signal ratio (I_{520}/I_{653}) of **DMBP** enhanced 40-fold within 1 min and reached equilibrium within 10 mins. Next, we evaluated the pH tolerance of **DMBP** and the reaction system, as shown in Fig. S12B, after the addition of 40.0 μM of HOBr, probe **DMBP** showed stable fluorescence emission of I_{520}/I_{653} under pH 3~12

that contained physiological conditions. The above results indicated that **DMBP** is an excellently sensitive and stable fluorescent probe to detect HOBr.

3.3. Validation of reaction mechanism

The electron donor *N, N-diethyl* and acceptor carbonyl groups exist in **DMBP** forming the ICT effect, and producing intense red fluorescence. According to the changes of fluorescence emission, the adding of HOBr caused significant reduction of intensity at 653 nm and increased at 520 nm, resulting in a blue shift of fluorescence spectra, which may be attributed to the bromine substituent reduced the electron density of the oxygen heterocycle.

It was reported that HOBr could attack the 5-position of coumarin and the 4'(5') position of rhodamine B to generate brominated products, and the 8-position of **DMBP** had similar substituents in the adjacent position with them [28]. Therefore, it was speculated that the electrophilic substitution of HOBr occurred at the 8-position of **DMBP** (Fig. 4A). After the electrophilic substitution reaction between **DMBP** and HOBr, the bromine replaced the hydrogen at the 8-position of probe, which effectively inhibited the ICT process, and triggered a blue shift of emission wavelength to produce a ratiometric fluorescence signal. For further confirmation of the mechanism, we subjected the reaction product to mass spectrometry and liquid phase analysis. Probe **DMBP** was dissolved in methanol at a final concentration of 10.00 μM, then detected with an injection volume of 10.00 μL. The eluent was methanol at a flow rate of 1 $mL \cdot min^{-1}$, probe **DMBP** (10.00 μM) was treated with HOBr (50.00 μM) for 10 min, signals were collected at 420 nm and 580 nm. As

shown in Fig. 4B, probe **DMBP** had a chromatographic peak at 7.9 min after isocratic elution with 85% methanol, and a new peak at 9.8 min appeared after the reaction with HOBr, which demonstrated the generation of new product. To further determine the structure of the new product, we purified and subjected it to mass spectrometry, the measured mass spectral peak was 562.0947 (Fig. S5), which was consistent with the calculated value of **DMBP-Br** as 562.0954, providing a proof of the generation of **DMBP-Br**. Subsequently, the synthesized **DMBP-Br** was subjected to liquid phase analysis, and the peak position was consistent with the reaction product, demonstrating that the probe reacted with HOBr to form **DMBP-Br**.

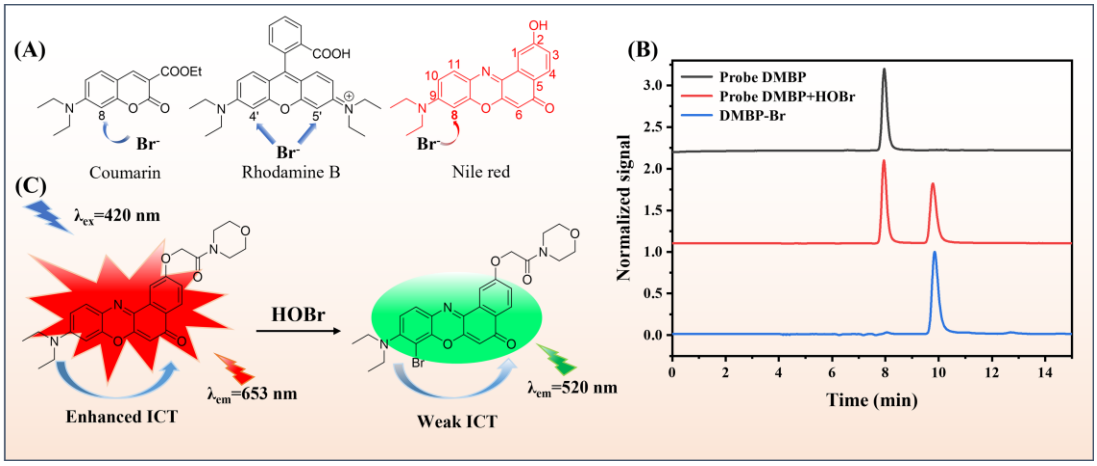

Fig. 4. (A) Prediction of reaction sites between probe **DMBP** and HOBr. (B) Liquid phase spectra before and after the reaction with HOBr. (C) Reaction mechanism between probe **DMBP** and HOBr.

3.4. Fluorescence imaging of HOBr in HepG2 cells

Before cell imaging, the toxicity of **DMBP** to HepG2 cells was assessed by MTT assay firstly (Fig. S10), more than 80% of HepG2 cells survived when the concentration of **DMBP** reached 12.50 μM, indicating that probe **DMBP** had lower cytotoxicity and was available for cell imaging.

There are many reactive oxygen species involved in reactions inside lysosomes,

so it is interesting to study the reactive oxygen species inside lysosomes. We attached a lysosomal localization motif to the designed probe and determined the localization of **DMBP** in the lysosome by co-localization imaging experiments. As shown in Fig. 5A, after co-incubation with Lyso-Tracker Green (a commercially available lysosomal green fluorescent probe) and **DMBP** with HepG2 cells for 3 min, the red fluorescence collected by the probe highly overlapped with the green fluorescence of Lyso-Tracker Green. In addition, the cross-sectional fluorescence intensity distributions of **DMBP** and Lyso-Tracker Green in the cells were essentially identical (Pearson coefficient was 0.97), indicating that probe **DMBP** could be localized in lysosomes.

Then the response of **DMBP** to exogenous HOBr in living cells was investigated. The green and red channels were set up for simultaneous detection, an obvious fluorescence signal could be observed in the red channel but almost none in the green channel when **DMBP** was incubated with cells (Fig. 5B). However, after the incubation of HOBr, the fluorescence of the red channel decreased and that of the green channel was significantly enhanced, indicating that **DMBP** could be used to detect exogenous HOBr. In addition, the fluorescence intensity changes of two channels were positively correlated with the concentration of HOBr, which suggested that **DMBP** could realize visualization of exogenous HOBr in living cells.

Some abnormal activities in the organism can change the concentration of HOBr in the lysosome, therefore, observing the change of endogenous HOBr is beneficial to determine the role it plays in the lysosome. Fig. 5C shows the fluorescence imaging experiment of **DMBP** on endogenous HOBr. HepG2 cells treated with **DMBP** only

showed red fluorescence, after the stimulation of NaBr to produce HOBr in cells, the fluorescence at red channel was weakened, while the fluorescence at the green channel was significantly enhanced, and this trend was correlated with the concentration of NaBr. Subsequently, the added reagent NAC (a scavenger of HOBr) decreased the green fluorescence signal significantly, which proved that the change of fluorescence signal at the green channel was caused by the generation of HOBr. In summary, probe **DMBP** can monitor the fluctuation of exogenous and endogenous HOBr in HepG2 cells in real time and is expected to be used to examine the role of HOBr in lysosomes.

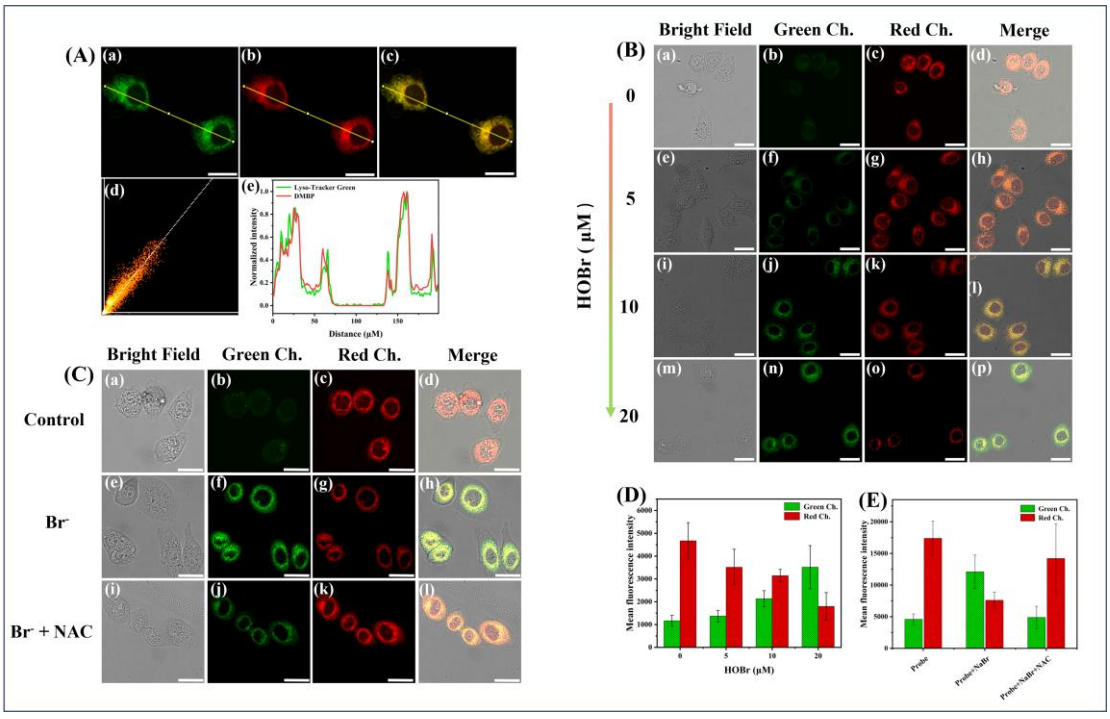

Fig. 5. (A) Co-localization images of Lysosomes. (a) Lyso-Tracker Green (1.00 μM), (b) **DMBP** (5.00 μM), (c) merged image. Green channel was acquired at 500~600 nm, λ_{ex} =488 nm, red channel was acquired at 610~750 nm, λ_{ex} = 552 nm. (d) Co-localization scatter plot of (a). (e) Cross section intensity of (a). (B) Confocal fluorescence images of HepG2 cells with **DMBP** (5.00 μM) and exogenous HOBr (0 μM, 5.00 μM, 10.00 μM, 20.00 μM). (C) Confocal fluorescence images of HepG2 cells with **DMBP** (5.00 μM) and endogenous HOBr. (a-d) control; (e-h) NaBr (20.00 μM); (i-l) NaBr (20.00 μM) and NAC (250.00 μM). (D) Digitization fluorescence intensity of each group of cells in (B). (E) Digitization fluorescence intensity of each group of cells in (C). Green channel was acquired at 480~600 nm, λ_{ex} =405 nm, red channel was acquired at 610~750

nm, λ_{ex} =552 nm, Scale bar: 25 μm.

3.5. Fluorescence imaging of HOBr in zebrafish

Given the relatively promising detection ability of probe **DMBP** in cells, we further explored its application in zebrafish. Using three-day zebrafish as animal model, we first investigated the fluorescence signal in zebrafish before and after the addition of exogenous HOBr. As shown in Fig. 6A, after incubation of **DMBP** with zebrafish alone, there was a clear fluorescence signal at red channel but almost not at green channel. Conversely, the zebrafish incubated with **DMBP** and different concentrations of HOBr showed gradually enhanced fluorescence signal at the green channel and decreased at the red channel. The above results demonstrate that probe **DMBP** can detect exogenous HOBr in animal models, further indicating its promising application for in vivo imaging.

EPO can catalyze a reaction to produce HOBr, making the concentration of HOBr correlate with EPO activity, which is associated with inflammation and tissue damage in vivo; therefore, detection of endogenous HOBr concentration is expected to enable monitoring of EPO activity for early diagnosis of diseases. Based on this information, we imaged endogenous HOBr (induced by NaBr) in zebrafish using probe **DMBP**. Enhanced green fluorescence and attenuated red fluorescence were observed in zebrafish treated with NaBr. To demonstrate that the change in fluorescence was caused by HOBr, we also made a control experiment using reagent NAC to eliminate the HOBr induced by NaBr, and as shown in the Fig. 6B, the green fluorescence was significantly weakened, demonstrating that the change in fluorescence of the green channel was caused by HOBr. The above experiments

manifested that probe **DMBP** is capable of detecting endogenous HOBr in organisms, and is expected to be used for early diagnosis of diseases.

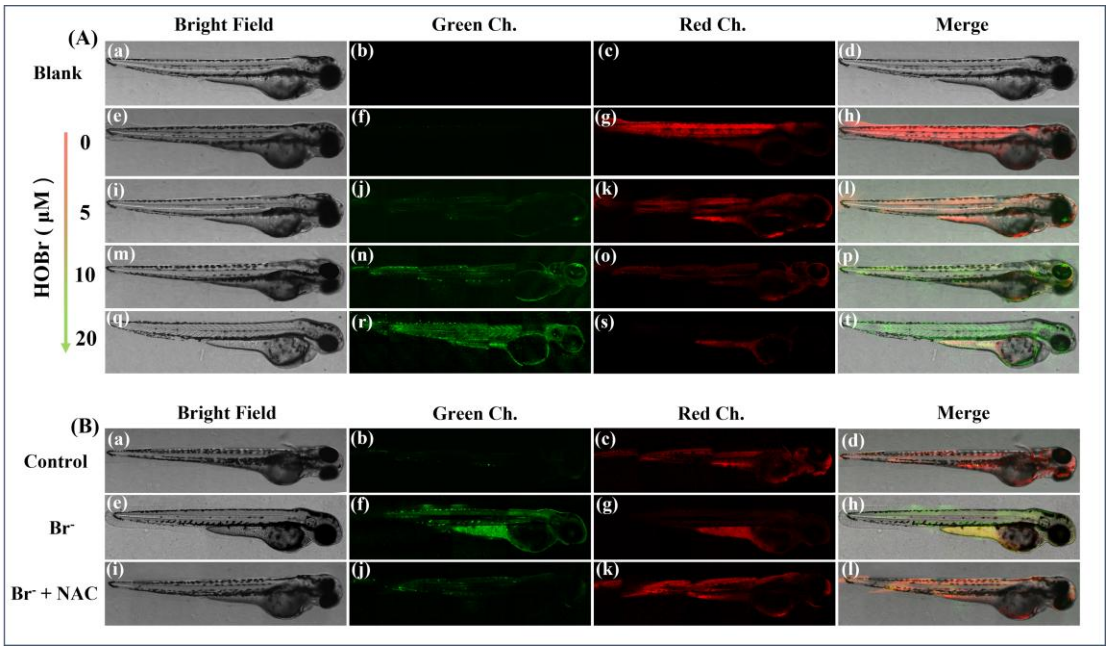

Fig. 6. (A) Confocal fluorescence images of zebrafish with probe **DMBP** (5.0 μM) and exogenous HOBr (0 μM, 5.00 μM, 10.00 μM, 20.00 μM). (B) Confocal fluorescence images of **DMBP** (5.00 μM) and endogenous HOBr in zebrafish. (a-d) control; (e-h) NaBr (20.00 μM); (i-l) NaBr (20.00 μM) and NAC (250.00 μM). Green channel was acquired at 480~600 nm, λ_{ex} =405 nm, red channel was acquired at 610~750 nm, λ_{ex} =552 nm.

4. Conclusion

In summary, we designed and synthesized a lysosome-targeted NIR fluorescent probe **DMBP** based on the Nile red skeleton. The experiment result shows that HOBr can react with the probe via electrophilic substitution, resulting in an increasing emission peak at 520 nm, which produced a ratiometric signal change from red to green depending on the change of ICT process. **DMBP** exhibits high selectivity and sensitivity to HOBr and can rapidly distinguish other ROS. **DMBP** also has good biocompatibility and cell permeability that had been successfully used for exogenous and endogenous HOBr imaging in HepG2 cells and zebrafish. More importantly, as the first NIR fluorescent probe can simultaneously localize lysosomes and achieve

ratiometric detection of HOBr, we believe that probe **DMBP** is a potential tool for the diagnosis of HOBr-related diseases in lysosomes.

CrediT authorship contribution statement

Wanqing Zhao: Conceptualization, Methodology, Data Curation, Writing - Original Draft, Writing-Review & Editing. **Pengyue Xu:** Methodology, Data Curation, Writing-Review & Editing. **Yixuan Ma:** Validation, Data Curation. **Yiming Song:** Supervision, Project administration, Conceptualization, Methodology, Writing-review & editing. **Yihang Wang:** Methodology, Investigation, Data Curation, Formal analysis. **Panpan Zhang:** Investigation, Data Curation, Formal analysis. **Bin Li:** Investigation, Data Curation, Formal analysis. **Yongmin Zhang:** Conceptualization, Writing-review & editing. **Jianli Li**: Data Curation, Conceptualization. **Shaoping Wu:** Supervision, Project administration, Conceptualization, Methodology, Writing-review & editing.

Declaration of Competing Interest

The authors declare that they have no known competing financial interests or personal relationships that could have appeared to influence the work reported in this paper.

Data availability

Data will be made available on request.

Acknowledgements

The authors thank the National Natural Science Foundation of China (No. 21572177), the Key Research and Development Program of Shaanxi Province (No.

2021ZDLSF03-03), Biomedicine Key Laboratory of Shaanxi Province (No. 2018SZS41).

Appendix A. Supplementary data

Supplementary data to this article can be found online at https://xxx

References

[1] S. Antonucci, F.D. Lisa, N. Kaludercic, Mitochondrial reactive oxygen species in physiology and disease, Cell Calcium. 94 (2021), 102344.

[2] Y. Dai, Y. Ding, L. Li, Nanozymes for regulation of reactive oxygen species and disease therapy, Chin Chem Lett. 32 (9) (2021) 2715-2728.

[3] X.-M. Cheng, Y.-Y. Hu, T. Yang, N. Wu, X.-N. Wang, Reactive oxygen species and oxidative stress in vascular-related diseases, Oxid. Med. Cell. Longev. 2022 (2022), 7906091.

[4] S.J. Weiss, S.T. Test, C.M. Eckmann, D. Roos, S. Regiani, Brominating oxidants generated by human eosinophils, Science. 234 (4773) (1986), 200-203.

[5] J. Wang, A. Slungaard, Role of eosinophil peroxidase in host defense and disease pathology, Arch. Biochem. 445 (2) (2006) 256-260.

[6] T. Suzuki, M. Kumagai, M. Furusawa, Effects of urea on the reactions of nucleosides with hypobromous acid, Chem. Pharm. Bull. 67 (7) (2019) 707-712.

[7] A.S. McCall, Christopher F. Cummings, G. Bhave, R. Vanacore, A. Page-McCaw, B.G. Hudson, Bromine is an essential trace element for assembly of collagen IV scaffolds in tissue development and architecture, Cell. 157 (6) (2014) 1380-1392.

[8] T. Suzuki, A. Okuyama, Reactions of rebamipide with hypobromous acid, Chem. Pharm. Bull. 67 (10) (2019) 1164-1167.

[9] Y.W. Yap, M. Whiteman, N.S. Cheung, Chlorinative stress: An under appreciated mediator of neurodegeneration?, Cell. Signal. 19 (2) (2007) 219-228.

[10] C. Gorrini, I.S. Harris, T.W. Mak, Modulation of oxidative stress as an anticancer strategy, Nat. Rev. Drug Discov. 12 (12) (2013) 931-947.

[11] K.L. Brown, C. Darris, K.L. Rose, O.A. Sanchez, H. Madu, J. Avance, N. Brooks, M.-Z. Zhang, A. Fogo, R. Harris, B.G. Hudson, P. Voziyan, Hypohalous acids contribute to renal

extracellular matrix damage in experimental diabetes, Diabetes. 64 (6) (2015) 2242-2253.

[12] T. Kurz, A. Terman, B. Gustafsson, U.T. Brunk, Lysosomes and oxidative stress in aging and apoptosis, Biochim Biophys Acta Gen Subj. 1780 (11) (2008) 1291-1303.

[13] Z. Dong, W. Liang, Y. Dong, H. Ren, Y. Wang, Water-soluble dual lysosome/mitochondria-targeted fluorescent probe for detection of SO_2 in water, food, herb, and live cells, Bioorg. Chem. 129 (2022), 106189.

[14] X. Duan, Q. Tong, C. Fu, L. Chen, Lysosome-targeted fluorescent probes: design mechanism and biological applications, Bioorg. Chem. 140 (2023), 106832.

[15] L. Guan, W. Hu, H. Zuo, H. Sun, Y. Ai, M.-H. He, C. Ma, M. Ding, Q. Liang, An NIR fluorescent/photoacoustic dual-mode probe of NADPH for tumor imaging, Chem. Commun. 59 (12) (2023) 1617-1620.

[16] X. Li, Q. Feng, L. Qu, T. Zhao, X. Li, T. Bai, S. Sun, S. Wu, Y. Zhang, J. Li, A water-soluble and incubate-free fluorescent environment-sensitive probe for ultrafast visualization of protein thiols within living cells, Anal Chim Acta. 1126 (2020) 72-81.

[17] S. Zhang, B. Li, J. Zhou, J. Shi, Z. He, Y. Zhao, Y. Li, Y. Shen, Y. Zhang, S. Wu, Kill three birds with one stone: mitochondria-localized tea saponin derived carbon dots with AIE properties for stable detection of HSA and extremely acidic pH, Food Chem. 405 (2023), 134865.

[18] Q. Feng, Y. Song, Y. Ma, Y. Deng, P. Xu, K. Sheng, Y. Zhang, J. Li, S. Wu, Molecular engineering of benzenesulfonyl analogs for visual hydrogen polysulfide fluorescent probes based on Nile red skeleton, Spectrochim. Acta A Mol. Biomol. Spectrosc. 296 (2023), 122658.

[19] H. Zhu, M. Liu, C. Liu, X. Li, K. Wang, M. Yu, W. Sheng, B. Zhu, A reversible and ratiometric fluorescent probe based on rhodol derivative with an ESIPT unit for monitoring copper ion content and in situ evaluation of related drugs in cells, Bioorg. Chem. 139 (2023), 106733.

[20] W.-J. Bi, Z.-X. Lan, X.-C. Wang, Y.-X. Cheng, J.-B. Jiang, Design and synthesis of photoaffinity-based probes for labeling β-glucuronidase, Bioorg. Chem. 141 (2023), 106909.

[21] K. Xu, H. Chen, J. Tian, B. Ding, Y. Xie, M. Qiang, B. Tang, A near-infrared reversible

fluorescent probe for peroxynitrite and imaging of redox cycles in living cells, Chem. Commun. 47 (33) (2011) 9468-9470.

[22] B. Wang, P. Li, F. Yu, J. Chen, Z. Qu, K. Han, A near-infrared reversible and ratiometric fluorescent probe based on Se-BODIPY for the redox cycle mediated by hypobromous acid and hydrogen sulfide in living cells, Chem. Commun. 49 (51) (2013) 5790-5792.

[23] F. Yu, P. Song, P. Li, B. Wang, K. Han, Development of reversible fluorescence probes based on redox oxoammonium cation for hypobromous acid detection in living cells, Chem. Commun. 48 (62) (2012) 7735-7737.

[24] T.I. Kim, B. Hwang, B. Lee, J. Bae, Y. Kim, Selective monitoring and imaging of eosinophil peroxidase activity with a J-aggregating probe, J. Am. Chem. Soc. 140 (37) (2018) 11771-11776.

[25] D. Zhang, X. Yang, T. Wang, X. Ji, X. Wu, Advances in organic fluorescent probes for bromide ions, hypobromous acid and related eosinophil peroxidase-A review, Anal. Chim. Acta. 1244 (2023), 340626.

[26] X. Huo, X. Wang, R. Yang, Z. Li, Y. Sun, L. Qu, H. Zeng, A novel fluorescent probe for highly selective and sensitive detection of hypobromous acid in arthritis model mice, Sens Actuators B Chem. 315 (2020), 128125.

[27] P. Jia, D. Liu, Z. Zhuang, L. Qu, C. Liu, Y. Zhang, Z. Li, H. Zhu, Y. Yu, X. Zhang, W. Sheng, B. Zhu, A highly selective ratiometric fluorescence probe for bioimaging of hypobromous acid in living cells and zebrafish, Sens Actuators B Chem. 320 (2020), 128583.

[28] L. Wu, Y. Shi, H. Yu, J. Zhang, Z. Li, X.-F. Yang, Bromination-induced spirocyclization of rhodamine dyes affording a FRET-based ratiometric fluorescent probe for visualization of hypobromous acid (HOBr) in live cells and zebrafish, Sens Actuators B Chem. 337 (2021), 129790.

[29] H. Zhu, P. Jia, X. Wang, Y. Tian, C. Liu, X. Li, K. Wang, P. Li, B. Zhu, B. Tang, In situ observation of lysosomal hypobromous acid fluctuations in the brain of mice with depression phenotypes by two-photon fluorescence imaging, Anal. Chem. 94 (34) (2022) 11783-11790.

[30] D.I. Pattison, M.J. Davies, Kinetic Analysis of the reactions of hypobromous acid with protein components: implications for cellular damage and use of 3-bromotyrosine as a

marker of oxidative stress, Biochemistry. 43 (16) (2004) 4799-4809.

[31] V.F. Ximenes, N.H. Morgon, A.R. de Souza, Hypobromous acid, a powerful endogenous electrophile: experimental and theoretical studies, J. Inorg. Biochem. 146 (2015) 61-68.

[32] S.-R. Liu, S.-P. Wu, Hypochlorous acid turn-on fluorescent probe based on oxidation of diphenyl selenide, Org. Lett. 15 (4) (2013) 878-881.

[33] S.T. Manjare, S. Kim, W.D. Heo, D.G. Churchill, Selective and sensitive superoxide detection with a new diselenide-based molecular probe in living breast cancer cells, Org. Lett. 16 (2) (2014) 410-412.

[34] C.L. Hawkins, M.J. Davies, The role of aromatic amino acid axidation, protein unfolding, and aggregation in the hypobromous acid-induced inactivation of trypsin inhibitor and lysozyme, Chem. Res. Toxicol. 18 (11) (2005) 1669-1677.

[35] Z. Peng, B. Zhang, Nanobubble labeling and imaging with a solvatochromic fluorophore nile red, Anal. Chem. 93 (46) (2021) 15315-15322.

[36] R. Sun, W. Wan, W. Jin, Y. Bai, Q. Xia, M. Wang, Y. Huang, L. Zeng, J. Sun, C. Peng, B. Jing, Y. Liu, Derivatizing nile red fluorophores to quantify the heterogeneous polarity upon protein aggregation in the cell, Chem. Commun. 58 (35) (2022) 5407-5410.

[37] H. Sun, Y. Du, X. Chen, H. Jiang, Y. Li, L. Shen, Design, synthesis, and evaluation of nile red analogs for myelin imaging as near-infrared fluorescence probe, Dyes Pigm. 208 (2022), 110804.

[38] X. Wang, L. Fan, X. Zhang, Q. Zan, W. Dong, S. Shuang, C. Dong, A red-emission fluorescent probe for visual monitoring of lysosomal pH changes during mitophagy and cell apoptosis, Analyst. 145 (21) (2020) 7018-7024.

[39] S. Biswas, T. Dutta, A. Silswal, R. Bhowal, D. Chopra, A.L. Koner, Strategic engineering of alkyl spacer length for a pH-tolerant lysosome marker and dual organelle localization, Chem. Sci. 12 (28) (2021) 9630-9644.